Soft, collinear, and nonrelativistic modes in radiative decays of very heavy quarkonium

Xavier Garcia i Tormo
Departament d'Estructura i Constituents de la Matèria, Universitat de Barcelona, Diagonal 647, E-08028 Barcelona, Catalonia, Spain

Joan Soto
Departament d'Estructura i Constituents de la Matèria, Universitat de Barcelona, Diagonal 647, E-08028 Barcelona, Catalonia, Spain and Institut de Ciències l'Espai–CSIC, Barcelona, Spain

(Received 9 February 2004; published 2 June 2004)

We analyze the end-point region of the photon spectrum in semi-inclusive radiative decays of very heavy quarkonium ($m\alpha_s^2 \gg \Lambda_{\rm QCD}$). We discuss the interplay of the scales arising in the soft-collinear effective theory, m, $m(1-z)^{1/2}$, and $m(1-z)$ for z close to 1, with the scales of heavy quarkonium systems in the weak coupling regime, m, $m\alpha_s$, and $m\alpha_s^2$. For $1-z \sim \alpha_s^2$ only collinear and (ultra)soft modes are seen to be relevant, but the recently discovered soft-collinear modes show up for $1-z \ll \alpha_s^2$. The S- and P-wave octet shape functions are calculated. When they are included in the analysis of the photon spectrum of the $\Upsilon(1S)$ system, the agreement with data in the end-point region becomes excellent. The nonrelativistic QCD matrix elements $\langle 1^3S_1|O_8(^1S_0)|1^3S_1\rangle$ and $\langle 1^3S_1|O_8(^3P_J)|1^3S_1\rangle$ are also obtained.

DOI: 10.1103/PhysRevD.69.114006 PACS number(s): 13.20.Gd, 12.38.Cy, 12.39.St

I. INTRODUCTION

Effective field theories (EFTs) have proved extremely useful in the field of strong interactions. Applications to high energy processes in QCD involving very energetic partons [1], however, have been elusive until recently. Important features of a suitable EFT for such processes were outlined in [2], which led to the development of the so called soft-collinear effective theory (SCET) [3–5] (see [6] for a pedagogical introduction).

The SCET has generated high expectations. Indeed, factorization proofs appear to be greatly simplified and power corrections seem to come under control. In addition, a large number of potential applications is envisaged [7]. Among these, exclusive and semi-inclusive B decays deserve special attention because of the necessity to have good control of the hadronic effects in order to extract the Cabibbo-Kobayashi-Maskawa matrix elements from the abundant B-factory data.

SCET was originally formulated in terms of soft, collinear, and ultrasoft modes. Later, it was realized that two possible scalings for collinear modes were relevant and the terminology $\mathrm{SCET_I}$ and $\mathrm{SCET_{II}}$ was introduced. Recently a new mode, called the soft-collinear mode, has been claimed to be necessary [5] (see [8] for the latest discussions). It is often assumed that some of the momentum components of these modes have typical sizes $\sim\Lambda_{\rm QCD}$ or even smaller.

One of the difficulties that one faces in B physics is that the bound state dynamics of the initial B meson is dominated by the scale $\Lambda_{\rm QCD}$, and hence a weak coupling analysis is not reliable. Therefore, the interplay of the initial bound state dynamics with final state modes of momentum components of the order of $\Lambda_{\rm QCD}$ (or smaller) is difficult to figure out. We advocate here that a very heavy quarkonium in the initial state may provide an excellent theoretical tool to shed light on this issue, since the bound state dynamics occurs at weak coupling and it is amenable to a detailed analysis. We shall illustrate this point by analyzing the end-point region of the photon spectrum in inclusive decays of very heavy quarkonium.

Semi-inclusive radiative decays for the $\Upsilon(1S)$ have already been discussed in the framework of SCET [9–11]. The SCET has been used to put forward factorization formulas and to resum Sudakov logarithms. An improved description of data [12] with respect to earlier approaches [13] has been achieved. However, the bound state dynamics, which is relevant for the evaluation of the octet shape functions, has not been studied in detail, but rather modeled by analogy with B-meson systems [14], which is a doubtful approximation. We shall calculate here the octet shape functions under the assumption that the bottom quark is sufficiently heavy as to consider $\Upsilon(1S)$ a Coulombic state. This assumption appears to be self-consistent in the calculation of the spectrum [15–18] and decay and production currents [19]. We observe that the factorization scale dependence of the shape functions is sensitive to the bound state dynamics and discuss its cancellation.

We organize the paper as follows. In Sec. II we calculate the photon spectrum at the end-point region in the weak coupling regime. We do so by first matching QCD to nonrelativistic QCD (NRQCD) [20] $+\mathrm{SCET_I}$, then NRQCD $+\mathrm{SCET_I}$ to potential NRQCD (pNRQCD) [21] $+\mathrm{SCET_{II}}$, and finally carrying out the calculations in the later EFT. We confirm the factorization formulas [10,11] and obtain the octet shape functions. In Sec. III, we apply our results to the $\Upsilon(1S)$ system and obtain a very good description of the experimental data [12] in the end-point region. In Sec. IV we discuss the interplay of the several scales in the problem, in particular the emergence of a soft-collinear mode. Section V is devoted to the conclusions. In the Appendix we present results for NRQCD octet matrix elements of the 1^3S_1 state, which follow from those of Sec. II.

II. THE END-POINT REGION OF THE PHOTON SPECTRUM

We start from the formulas given in Ref. [11]:

$$\frac{d\Gamma}{dz} = z\frac{M}{16\pi^2}\,\mathrm{Im}\,T(z),$$

$$T(z) = -i\int d^4x e^{-iq\cdot x} \times \langle n^{2S+1}L_J|T\{J_\mu(x)J_\nu(0)\}|n^{2S+1}L_J\rangle\,\eta_\perp^{\mu\nu} \quad (1)$$

where $J_\mu(x)$ is the electromagnetic current for heavy quarks in QCD and we have used spectroscopic notation for the heavy quarkonium states. The formula above holds for states satisfying relativistic normalization. In the case that nonrelativistic normalization is used, as we shall do below, the right-hand side of either the first or second formula in Eq. (1) must be multiplied by $2M$, M being the mass of the heavy quarkonium state. In the end-point region the photon momentum (in light cone coordinates) in the rest frame of the heavy quarkonium is $q=(q_+,q_-,q_\perp)=(zM/2,0,0)$ with $z\sim 1$ $(M\sqrt{1-z}\ll M)$. This together with the fact that the heavy quarkonium is a nonrelativistic system fixes the relevant kinematic situation. It is precisely in this situation when the standard NRQCD factorization (operator product expansion) breaks down [22]. The quark (antiquark) momentum in the $Q\overline{Q}$ rest frame can be written as $p=(p_0,\mathbf{p})$, $p_0=m+l_0$, $\mathbf{p}=\mathbf{l}$; $l_0,\mathbf{l}\ll m$, m being the mass of the heavy quark $(M\sim 2m)$. Momentum conservation implies that if a few gluons are produced in the short distance annihilation process at least one of them has momentum $r=(r_+,r_-,r_\perp)$, $r_-\sim M/2$, $r_+,r_\perp\ll M$, which we will call collinear. At short distances, the emission of hard gluons is penalized by $\alpha_s(m)$ and the emission of softer ones by powers of the soft scale over M. Hence, the leading contribution at short distances consists of the emission of a single collinear gluon. This implies that the $Q\overline{Q}$ pair must be in a color octet configuration, which means that the full process will have an extra long distance suppression related to the emission of (ultra) soft gluons. The next-to-leading contribution at short distances already allows for a singlet $Q\overline{Q}$ configuration. Hence, the relative weight of color singlet and color octet configurations depends not only on z but also on the bound state dynamics, and it is difficult to establish *a priori*. In order to do so, it is advisable to implement the constraints above by introducing suitable EFTs. In the first stage we need NRQCD [20], which factors out the scale m in the $Q\overline{Q}$ system, supplemented by collinear gluons, namely, gluons for which the scale m has been factored out from the components $r_+,r_\perp$ (but is still active in the component r_-). For the purposes of this work it is enough to take for the Lagrangian of the collinear gluons the full QCD Lagrangian and enforce $r_+,r_\perp\ll m$ when necessary.

A. Matching QCD to NRQCD + SCET$_\mathrm{I}$

For definiteness, we shall restrict our analysis to $^3S_1$ states, which decay mainly through two additional gluons. At the tree level, the electromagnetic current in Eq. (1) can be matched to the following currents[1] in this EFT [11]:

$$J_\mu(x) = e^{-i2mx_0}[\Gamma^{(1,^3S_1)}_{\alpha\beta i\mu}J^{i\alpha\beta}_{(1,^3S_1)}(x) + \Gamma^{(8,^1S_0)}_{\alpha\mu}J^{\alpha}_{(8,^1S_0)}(x) + \Gamma^{(8,^3P_J)}_{\alpha\mu ij}J^{\alpha ij}_{(8,^3P_J)}(x)+\cdots] + \mathrm{H.c.}, \quad (2)$$

$$\Gamma^{(1,^3S_1)}_{\alpha\beta i\mu} = \frac{g_s^2 ee_Q}{3m^2}\,\eta^\perp_{\alpha\beta}\eta_{\mu i},$$

$$J^{i\alpha\beta}_{(1,^3S_1)}(x) = \chi^\dagger\boldsymbol{\sigma}^i\psi\,\mathrm{Tr}\{B^\alpha_\perp B^\beta_\perp\}(x),$$

$$\Gamma^{(8,^1S_0)}_{\alpha\mu} = \frac{g_s ee_Q}{m}\boldsymbol{\epsilon}^\perp_{\alpha\mu}, \quad J^{\alpha}_{(8,^1S_0)}(x) = \chi^\dagger B^\alpha_\perp\psi(x),$$

$$\Gamma^{(8,^3P_J)}_{\alpha\mu ij} = \frac{g_s ee_Q}{m^2}(\eta^\perp_{\alpha j}\eta^\perp_{\mu i}+\eta^\perp_{\alpha i}\eta^\perp_{\mu j}-\eta^\perp_{\alpha\mu}n^j n^i),$$

$$J^{\alpha ij}_{(8,^3P_J)}(x) = -i\chi^\dagger B^\alpha_\perp\boldsymbol{\nabla}^i\boldsymbol{\sigma}^j\psi(x), \quad (3)$$

where $n=(n_+,n_-,n_\perp)=(1,0,0)$ and $\boldsymbol{\epsilon}^\perp_{\alpha\mu}=\boldsymbol{\epsilon}_{\alpha\mu\rho 0}n^\rho$. These effective currents can be identified with the leading order in α_s of the currents introduced in [11]. We use both latin (1 to 3) and greek (0 to 3) indices, $B^\alpha_\perp$ is a single collinear gluon field here, and ee_Q is the charge of the heavy quark. Note, however, that in order to arrive at Eq. (2) one need not specify the scaling of collinear fields as $M(\lambda^2,1,\lambda)$ but only the cutoffs mentioned above, namely, $r_+,r_\perp\ll M$. Even though the P-wave octet piece appears to be $1/m$ suppressed with respect to the S-wave octet piece, it will eventually give rise to contributions of the same order once the bound state effects are taken into account. This is due to the fact that the $^3S_1$ initial state needs a chromomagnetic transition to become an octet $^1S_0$, which is α_s suppressed with respect to the chromoelectric transition required to become an octet ^3P_J.

$T(z)$ can then be written as

$$T(z) = H^{(1,^3S_1)}_{ii'\alpha\alpha'\beta\beta'}T^{ii'\alpha\alpha'\beta\beta'}_{(1,^3S_1)} + H^{(8,^1S_0)}_{\alpha\alpha'}T^{\alpha\alpha'}_{(8,^1S_0)} + H^{(8,^3P_J)}_{\alpha ij\alpha' i' j'}T^{\alpha ij\alpha' i' j'}_{(8,^3P_J)}+\cdots, \quad (4)$$

where

$$H^{(1,^3S_1)}_{ii'\alpha\alpha'\beta\beta'} = \eta^{\mu\nu}_\perp\Gamma^{(1,^3S_1)}_{\alpha\beta i\mu}\Gamma^{(1,^3S_1)}_{\alpha'\beta' i'\nu},$$

$$H^{(8,^1S_0)}_{\alpha\alpha'} = \eta^{\mu\nu}_\perp\Gamma^{(8,^1S_0)}_{\alpha\mu}\Gamma^{(8,^1S_0)}_{\alpha'\nu},$$

$$H^{(8,^3P_J)}_{\alpha ij\alpha' i' j'} = \eta^{\mu\nu}_\perp\Gamma^{(8,^3P_J)}_{\alpha\mu ij}\Gamma^{(8,^3P_J)}_{\alpha'\nu i' j'}, \quad (5)$$

[1]One-loop matching calculations are already available, analytical for the octet currents [23] and numerical for the singlet one [24].

and

$$T^{ii'\alpha\alpha'\beta\beta'}_{(1,^3S_1)}(z) = -i\int d^4x e^{-iq\cdot x - 2mx_0}\langle\, ^3S_1|T\{J^{i\alpha\beta}_{(1,^3S_1)}(x)^\dagger \times J^{i'\alpha'\beta'}_{(1,^3S_1)}(0)\}|^3S_1\rangle,$$

$$T^{\alpha\alpha'}_{(8,^1S_0)}(z) = -i\int d^4x e^{-iq\cdot x - 2mx_0}\langle\, ^3S_1|T\{J^{\alpha}_{(8,^1S_0)}(x)^\dagger \times J^{\alpha'}_{(8,^1S_0)}(0)\}|^3S_1\rangle,$$

$$T^{\alpha ij\alpha' i' j'}_{(8,^3P_J)}(z) = -i\int d^4x e^{-iq\cdot x - 2mx_0}\langle\, ^3S_1|T\{J^{\alpha ij}_{(8,^3P_J)}(x)^\dagger \times J^{\alpha' i' j'}_{(8,^3P_J)}(0)\}|^3S_1\rangle. \quad (6)$$

In Eq. (4) we have not written a crossed term $(8,{}^1S_0\text{-}{}^3P_J)$ since it eventually vanishes at the order we will be calculating.

B. Matching NRQCD + SCET$_{\rm I}$ to pNRQCD + SCET$_{\rm II}$

If we restrict ourselves to z such that $M(1-z)\lesssim m\alpha_s^2$, the scale of the binding energy, we can proceed one step further in the EFT hierarchy. As discussed in Ref. [21], NRQCD still contains quarks and gluons with energies $\sim m\alpha_s$, which, in the situation above can be integrated out. This leads to potential NRQCD. On the SCET side, the restriction above implies that one may also restrict collinear gluons in the final state to have $r_+, r_\perp \ll M\sqrt{1-z}\lesssim m\alpha_s$, as we shall do. The scale $M\sqrt{1-z}$, which is still active in SCET$_{\rm I}$, must then be integrated out [9]. The integration of this scale produces the dominant contributions from the color singlet currents. We have

$$\langle\, ^3S_1|T\{J^{i\alpha\beta}_{(1,^3S_1)}(x)^\dagger J^{i'\alpha'\beta'}_{(1,^3S_1)}(0)\}|^3S_1\rangle \to 2N_c S_V^{i\,\dagger}(\mathbf{x},\mathbf{0},x_0)S_V^{i'}(\mathbf{0},\mathbf{0},0) \times\langle \mathrm{vac}|\mathrm{Tr}\{B_\perp^\alpha B_\perp^\beta\}(x)\mathrm{Tr}\{B_\perp^{\alpha'}B_\perp^{\beta'}\}(0)|\mathrm{vac}\rangle. \quad (7)$$

The calculation of the vacuum correlator for collinear gluons above has been carried out in [11], and the final result, which is obtained by sandwiching Eq. (7) between the quarkonium states, reduces to the one put forward in that reference.

For the color octet currents, the leading contribution arises from a tree level matching of the currents (2),

$$J^\alpha_{(8,^1S_0)}(x)\to\sqrt{2T_F}\,O_P^a(\mathbf{x},\mathbf{0},x_0)B_\perp^{a\alpha}(x),$$

$$J^{\alpha ij}_{(8,^3P_J)}(x)\to\sqrt{2T_F}[i\boldsymbol{\nabla}^i_{\mathbf{y}}O_V^{aj}(\mathbf{x},\mathbf{y},x_0)]\big|_{\mathbf{y}=\mathbf{0}}B_\perp^{a\alpha}(x). \quad (8)$$

S_V^i, O_V^{ai}, and O_P^a are the projections of the singlet and octet wave function fields introduced in [21] to their vector and pseudoscalar components, namely, $S=(S_P+S_V^i\sigma^i)/\sqrt{2}$ and $O^a=(O_P^a+O_V^{ai}\sigma^i)/\sqrt{2}$. $T_F=1/2$ and $N_c=3$ is the number of colors. $B_\perp^{a\alpha}(x)$ in Eq. (8) are now collinear gluons with $r_+, r_\perp \ll M\sqrt{1-z}\lesssim m\alpha_s$.

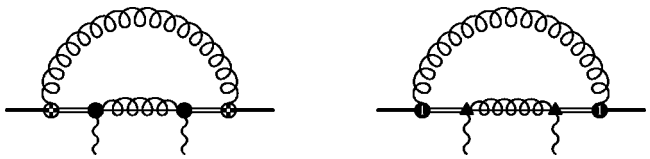

FIG. 1. Color octet contributions. ● represents the color octet S-wave current, ▲ represents the color octet P-wave current. The notation for the other vertices is that of Ref. [25], namely, ✤$:=(igc_F/\sqrt{N_cT_F})(\boldsymbol{\sigma}_1-\boldsymbol{\sigma}_2)/2m\,\mathrm{Tr}[T^b\mathbf{B}]$ and ❶$:=(ig/\sqrt{N_cT_F})\mathbf{x}\,\mathrm{Tr}[T^b\mathbf{E}]$. The solid line represents the singlet field, the double line represents the octet field, and the gluon with a line inside represents a collinear gluon.

C. Calculation in pNRQCD + SCET$_{\rm II}$

We shall now calculate the contributions of the color octet currents in pNRQCD coupled to collinear gluons. They are depicted in Fig. 1. For the contribution of the P-wave current, it is enough to have the pNRQCD Lagrangian at leading (nontrivial) order in the multipole expansion given in [21]. For the contribution of the S-wave current, one needs a $1/m$ chromomagnetic term given in [25].

Let us consider the contribution of the S-wave color octet current in some detail. We have from the first diagram of Fig. 1

$$T^{\alpha\alpha'}_{(8,^1S_0)}(z) = -i\,\eta_\perp^{\alpha\alpha'}(4\pi)\frac{32}{3}T_F^2\left(\frac{c_F}{2m}\right)^2\alpha_s(\mu_u)C_f \times\int d^3\mathbf{x}\int d^3\mathbf{x}'\,\psi^*_{n0}(\mathbf{x}')\psi_{n0}(\mathbf{x}) \times\int\frac{d^4k}{(2\pi)^4}\frac{\mathbf{k}^2}{k^2+i\epsilon}\left(\frac{1}{-k_0+E_n-h_o+i\epsilon}\right)_{\mathbf{x}',\mathbf{0}} \times\frac{1}{[M(1-z)-k_+]M-\mathbf{k}_\perp^2+i\epsilon} \times\left(\frac{1}{-k_0+E_n-h_o+i\epsilon}\right)_{\mathbf{0},\mathbf{x}}, \quad (9)$$

where we have used the Coulomb gauge (for both ultrasoft and collinear gluons). $E_n<0$ is the binding energy ($M=2m+E_n$) of the heavy quarkonium, $\psi_{n0}(\mathbf{x})$ its wave function, and h_o the color octet Hamiltonian at leading order, which contains the kinetic term and a repulsive Coulomb potential [21]. c_F is the hard matching coefficient of the chromomagnetic interaction in NRQCD [20], which will eventually be taken to 1. We have also enforced that k is ultrasoft by neglecting it in front of M in the collinear gluon propagator. We shall evaluate (9) in light cone coordinates. If we carry out first the integration over k_-, only the pole $k_-=\mathbf{k}_\perp^2/k_+$ contributes. Then the only remaining singularities

in the integrand are in the collinear gluon propagator. Hence, the absorptive piece can come only from its pole $M^2(1-z) - Mk_+ = \mathbf{k}_\perp^2$. If $k_+ \lesssim M(1-z)$, then $\mathbf{k}_\perp^2 \sim M^2(1-z)$, which implies $k_- \sim M$. This contradicts the assumption that k is ultrasoft. Hence, $\mathbf{k}_\perp^2$ must be expanded in the collinear gluon propagator. We then have

$$\begin{aligned}
&\mathrm{Im}[T^{\alpha\alpha'}_{(8,^1S_0)}(z)] \\
&= -\eta_\perp^{\alpha\alpha'}(4\pi)\frac{32}{3}T_F^2\left(\frac{c_F}{2m}\right)^2\alpha_s(\mu_u)C_f \\
&\times\int d^3\mathbf{x}\int d^3\mathbf{x}'\,\psi^*_{n0}(\mathbf{x}')\psi_{n0}(\mathbf{x})\frac{1}{8\pi M} \\
&\times\int_0^\infty dk_+\,\delta(M(1-z)-k_+) \\
&\times\int_0^\infty dx\left(\left\{\delta(\hat{\mathbf{x}}),\frac{h_o-E_n}{h_o-E_n+k_+/2+x}\right\}\right. \\
&\left.-\frac{h_o-E_n}{h_o-E_n+k_+/2+x}\,\delta(\hat{\mathbf{x}})\,\frac{h_o-E_n}{h_o-E_n+k_+/2+x}\right)_{\mathbf{x},\mathbf{x}'}
\end{aligned} \tag{10}$$

where we have introduced the change of variables $|\mathbf{k}_\perp| = \sqrt{2k_+x}$. Restricting ourselves to the ground state ($n=1$) and using the techniques of Ref. [26], we obtain

$$\begin{aligned}
\mathrm{Im}[T^{\alpha\alpha'}_{(8,^1S_0)}(z)] &= -\eta_\perp^{\alpha\alpha'}\frac{16}{3}T_F^2\left(\frac{c_F}{2m}\right)^2\alpha_s(\mu_u)C_f\frac{1}{M} \\
&\times\int_0^\infty dk_+\,\delta(M(1-z)-k_+) \\
&\times\int_0^\infty dx\left[2\psi_{10}(\mathbf{0})I_S\left(\frac{k_+}{2}+x\right)\right. \\
&\left.-I_S^2\left(\frac{k_+}{2}+x\right)\right],
\end{aligned}$$

$$\begin{aligned}
I_S\left(\frac{k_+}{2}+x\right) &:= \int d^3\mathbf{x}\psi_{10}(\mathbf{x})\left(\frac{h_o-E_1}{h_o-E_1+k_+/2+x}\right)_{\mathbf{x},\mathbf{0}} \\
&= m\sqrt{\frac{\gamma}{\pi}}\frac{\alpha_s N_c}{2}\frac{1}{1-z'}\left[1-\frac{2z'}{1+z'^2}\right. \\
&\left.\times F_1\left(-\frac{\lambda}{z'},1,1-\frac{\lambda}{z'},\frac{1-z'}{1+z'}\right)\right],
\end{aligned} \tag{11}$$

where

$$\gamma=\frac{mC_f\alpha_s}{2},\quad z'=\frac{\kappa}{\gamma},\quad -\frac{\kappa^2}{m}=E_1-\frac{k_+}{2}-x,$$

$$\lambda=-\frac{1}{2N_cC_f} \tag{12}$$

$[E_1=-m(C_f\alpha_s)^2/4=-\gamma^2/m]$. This result can be recast in the factorized form given in [11]:

$$\begin{aligned}
\mathrm{Im}[T^{\alpha\alpha'}_{(8,^1S_0)}(z)] &= -\eta_\perp^{\alpha\alpha'}\int dl_+ S_S(l_+) \\
&\times \mathrm{Im}\,J_M[l_+-M(1-z)],
\end{aligned}$$

$$\mathrm{Im}\,J_M[l_+-M(1-z)] = T_F^2(N_c^2-1)\frac{2\pi}{M}\delta(M(1-z)-l_+),$$

$$\begin{aligned}
S_S(l_+) &= \frac{4\alpha_s(\mu_u)}{3\pi N_c}\left(\frac{c_F}{2m}\right)^2\int_0^\infty dx\left[2\psi_{10}(\mathbf{0})I_S\left(\frac{l_+}{2}+x\right)\right. \\
&\left.-I_S^2\left(\frac{l_+}{2}+x\right)\right].
\end{aligned} \tag{13}$$

We have thus obtained the S-wave color octet shape function $S_S(l_+)$. Analogously, for the P-wave color octet shape functions, we obtain from the second diagram of Fig. 1

$$\begin{aligned}
\mathrm{Im}[T^{\alpha ij\alpha' i' j'}_{(8,^3P_J)}(z)] &= -\eta_\perp^{\alpha\alpha'}\delta^{jj'}\int dl_+\left[\delta_\perp^{ii'}S_{P1}(l_+)\right. \\
&\left.+\left(n^i n^{i'}-\frac{1}{2}\delta_\perp^{ii'}\right)S_{P2}(l_+)\right] \\
&\times \mathrm{Im}\,J_M[l_+-M(1-z)],
\end{aligned}$$

$$S_{P1}(l_+) := \frac{\alpha_s(\mu_u)}{6\pi N_c}\int_0^\infty dx\left[2\psi_{10}(\mathbf{0})I_P\left(\frac{l_+}{2}+x\right)-I_P^2\left(\frac{l_+}{2}+x\right)\right],$$

$$\begin{aligned}
S_{P2}(l_+) &:= \frac{\alpha_s(\mu_u)}{6\pi N_c}\int_0^\infty dx\,\frac{8l_+x}{(l_++2x)^2} \\
&\times\left[\psi_{10}^2(\mathbf{0})-2\psi_{10}(\mathbf{0})I_P\left(\frac{l_+}{2}+x\right)+I_P^2\left(\frac{l_+}{2}+x\right)\right],
\end{aligned} \tag{14}$$

where

$$\begin{aligned}
I_P\left(\frac{k_+}{2}+x\right) &:= -\frac{1}{3}\int d^3\mathbf{x}\mathbf{x}^i\psi_{10}(\mathbf{x})\left(\frac{h_o-E_1}{h_o-E_1+k_+/2+x}\nabla^i\right)_{\mathbf{x},\mathbf{0}} \\
&= \sqrt{\frac{\gamma^3}{\pi}}\frac{8}{3}(2-\lambda)\frac{1}{4(1+z')^3}\left(2(1+z')(2+z')\right. \\
&+(5+3z')(-1+\lambda)+2(-1+\lambda)^2 \\
&+\frac{1}{(1-z')^2}\left\{4z'(1+z')(z'^2-\lambda^2)\right. \\
&\times\left[-1+\frac{\lambda(1-z')}{(1+z')(z'-\lambda)}\right. \\
&\left.\left.\left.+{}_2F_1\left(-\frac{\lambda}{z'},1,1-\frac{\lambda}{z'},\frac{1-z'}{1+z'}\right)\right]\right\}\right).
\end{aligned} \tag{15}$$

Note that two shape functions are necessary for the *P*-wave case. The three shape functions above are UV divergent and need regularization and renormalization. In order to regulate them at this order it is enough to calculate the ultrasoft loop [the integral over k in Eq. (9)] in D dimensions (leaving the bound state dynamics in three space dimensions). The UV behavior can easily be obtained by making an expansion of I_S and I_P in $1/z'$, which is displayed in formulas (A3) and (A4) of the Appendix. For the purpose of this section we only need the expansions up to order $1/z'^2$. The singular pieces read $(D=4-2\varepsilon)$

$$S_S(l_+)|_{\varepsilon\to 0}\simeq \frac{4c_F^2\alpha_s(\mu_u)\gamma^5}{3\pi^2 N_c m^3}(1-\lambda)[-2+\lambda(2\ln 2+1)] \times\left[\frac{1}{\varepsilon}+\ln\left(\frac{\mu}{l_+/2+\gamma^2/m}\right)+\cdots\right],$$

$$S_{P1}(l_+)|_{\varepsilon\to 0}\simeq \frac{4\alpha_s(\mu_u)\gamma^5}{9\pi^2 N_c m}(2-\lambda)\left[-\frac{17}{6}+\lambda\left(2\ln 2+\frac{1}{6}\right)\right] \times\left[\frac{1}{\varepsilon}+\ln\left(\frac{\mu}{l_+/2+\gamma^2/m}\right)+\cdots\right],$$

$$S_{P2}(l_+)|_{\varepsilon\to 0}\simeq \frac{\alpha_s(\mu_u) l_+\gamma^3}{3\pi^2 N_c}\left[\frac{1}{\varepsilon}+\ln\left(\frac{\mu}{l_+}\right)+\cdots\right]. \quad (16)$$

The renormalization is not straightforward. We will assume that suitable operators exists which may absorb the $1/\varepsilon$ poles so that a minimal subtraction (MS) scheme makes sense to define the above expressions and discuss in the following the origin of such operators. In order to understand the scale dependence of Eq. (16) it is important to notice that it appears because the term $\mathbf{k}_\perp^2$ in the collinear gluon propagator is neglected in Eq. (9). It should then cancel with an IR divergence induced by keeping the term $\mathbf{k}_\perp^2$, which implies assuming a size $M^2(1-z)$ for it and expanding the ultrasoft scales accordingly. We have checked that it does. However, this contribution cannot be computed reliably within pNRQCD (nor within NRQCD) because it implies that the k_- component of the ultrasoft gluon is of order M, and hence it becomes collinear. A reliable calculation involves (at least) two steps within the EFT strategy. The first one is the matching calculation of the singlet electromagnetic current at higher orders both in α_s and in $(\mathbf{k}_\perp/M)^2$ and k_+/M. The second is a one-loop calculation with collinear gluons involving the higher order singlet currents. Notice, before going on, that all divergences (and logarithms) of $S_S(l_+)$ and $S_{P1}(l_+)$ in Eq. (16) are sensitive to the bound state dynamics, whereas those for $S_{P2}(l_+)$ are not. For the former, Fig. 2 shows the relevant diagrams which contribute to the IR behavior we are eventually looking for. We need next-to-next-to-leading order (NNLO) in α_s, but only LO in the $(\mathbf{k}_\perp/M)^2$ and k_+/M expansion. These diagrams are IR finite, but they induce, in the second step, the IR behavior which matches the UV of Eq. (16). The second step amounts to integrating

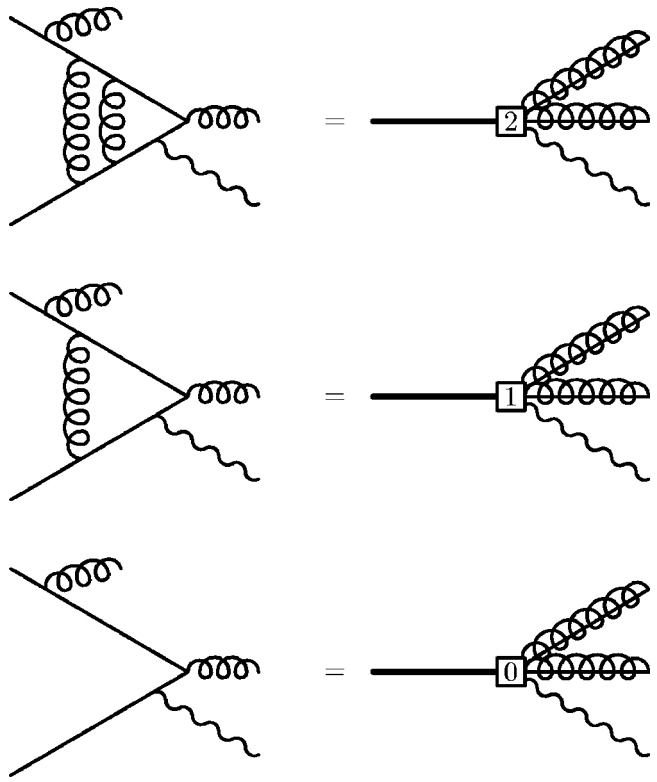

FIG. 2. Relevant diagrams in the matching calculation QCD $\to$pNRQCD+SCET.

out the scale $M\sqrt{1-z}$ by calculating the loops with collinear gluons and expanding smaller scales in the integrand. We have displayed in Fig. 3 the two diagrams that provide the aforementioned IR divergences. For the latter, the UV behavior of which does not depend on the bound state dynamics, we need the matching at LO in α_s (last diagram in Fig. 2) but NLO in k_+/M and $(\mathbf{k}_\perp/M)^2$. We have checked that the coefficient of the logarithm coincides with that of the $(1-z)\log(1-z)$ term in the QCD calculation [13], as it should.

The above means that the scale dependence of the leading order contributions of the color octet currents is of the same order as the NNLO contributions in α_s of the color singlet current, a calculation which is not available. One might, alternatively, attempt to resum logs and use the NLO calculation [24] as the boundary condition. This log resummation is nontrivial. One must take into account the correlation of scales inherent in the nonrelativistic system [27], which in the framework of pNRQCD has been implemented in [28,29], and combine it with the resummation of Sudakov logs in the framework of SCET [2,9–11] (see also [30]). Correlations within the various scales of SCET may start playing a role here as well [31]. In any case, it should be clear that by resumming only Sudakov logs, as has been

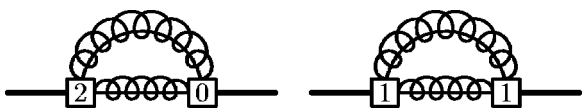

FIG. 3. Diagrams that induce an IR scale dependence which cancels against the UV one of the octet shape functions.

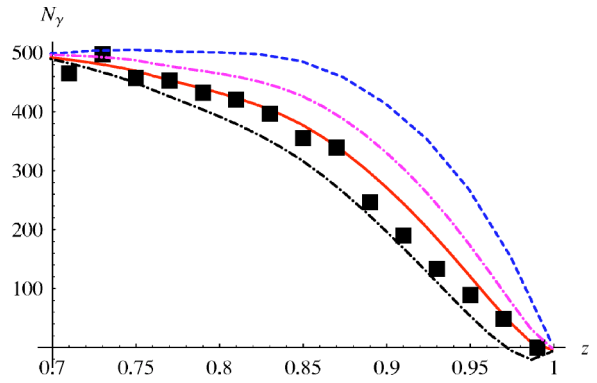

FIG. 4. End-point region of the photon spectrum in semi-inclusive Υ decay. The points are the CLEO data [12], the dashed line is the curve obtained in [11], and the solid and dot-dashed lines are our results. The solid line is obtained by setting $\mu = M\sqrt{(1-z)}$ (natural choice) and the dot-dashed lines are obtained by setting $\mu = 2M\sqrt{1-z}$ and $\mu = 2^{-1}M\sqrt{1-z}$.

done so far [9], one does not resum all the logs arising in the color octet contributions of heavy quarkonium, at least in the weak coupling regime.

III. APPLICATION TO THE $\Upsilon(1S)$

We apply here the results of Sec. II to the $\Upsilon(1S)$. There is good evidence that the $\Upsilon(1S)$ state can be understood as a weak coupling (positroniumlike) bound state [15–18]. Hence, ignoring $O(\Lambda_{\rm QCD})$ in the shape functions, as we did in Sec. II, should be a reasonable approximation. In the analysis of [11] the effects of the octet shape functions were set to zero, so we expect to improve on their results. We plot in Fig. 4 the CLEO data in the end-point region [12], the curve obtained in [11] (dashed line), and our curves (solid and dot-dashed lines). Our curves are obtained by adding to the results of [11], which consist of the leading log (LL) resummation of the singlet contributions only, our (MS) results for the color octet contributions (without LL resummation [9]) and setting the scale dependence to $\mu = M\sqrt{1-z}$ (solid line) and to $\mu = 2^{\pm 1}M\sqrt{1-z}$ (dot-dashed lines). The first choice is the most reasonable one according to the discussion in the previous section, and the last ones are displayed in order to get the flavor of the systematic errors. We have used the following values for the masses and α_s in our plots: $m_b = 4.8$ GeV, $M_\Upsilon = 9.46$ GeV, $\alpha_s(\mu_h) = 0.216$, $\alpha_s(\mu_s) = 0.32$, and $\alpha_s(\mu_u) = 0.65$. $\mu_h \sim m$ stands for the hard scale and is to be used for the α_s arising from Eq. (3). $\mu_s \sim m\alpha_s$ stands for the soft scale and is to be used for the α_s participating in the bound state dynamics [in E_1, I_S, I_P, and $\psi_{10}(\mathbf{0})$]. $\mu_u \sim m\alpha_s^2$ stands for the ultrasoft scale and is to be used for the α_s arising from the coupling of ultrasoft gluons. It turns out that the color octet contribution is numerically enhanced and dominates over the color singlet one in the whole end-point region. In order to compare with the experimental curve, the theoretical result must be convoluted with the experimental efficiency [12] and the overall normalization must be taken as a free parameter. By adjusting our curves to data around $z \sim 0.7$, we obtain an almost perfect agreement in the whole end-point region ($z \in [0.7,1]$) for $\mu = M\sqrt{1-z}$ (solid line). A complete analysis, including systematic errors, is beyond the scope of this paper. It would require either a NNLO matching or a NLO one [24] with next-to-leading log (NLL) resummation of the singlet current. In addition, one should estimate what the leading non-perturbative effects are. In any case, it should be clear from our results that the introduction of a gluon mass [32] is not necessary for the description of the experimental data on the photon spectrum in the end-point region of $\Upsilon(1S)$ radiative decays.

IV. DISCUSSION

We would like to make a few remarks which stem from the details of our calculation. In the existing formulations of SCET, suitable scaling properties are assigned to the various modes. However, the standard assignments are violated in our case. The collinear gluons in Fig. 1 scale as $m(\lambda^2,1,\lambda^2)$ rather than $m(\lambda^2,1,\lambda)$ ($\lambda = \sqrt{1-z}$), which is the assigned scaling in [3–5]. This indicates that the SCET should better be discussed in terms of UV (and IR) cutoffs for the relevant modes, rather than scaling properties. This becomes particularly clear when we analyze the scaling of the ultrasoft gluon in the same diagrams. If $m\alpha_s^2 \sim M(1-z)$, it scales like $m(\lambda^2,\lambda^2,\lambda^2)$ ($\lambda = \alpha_s$), which coincides with the standard scaling rules. If, however, $m\alpha_s^4 \sim M(1-z)$, it scales like $m(\lambda^4,\lambda^2,\lambda^3)$, the typical scaling of the recently discovered soft-collinear modes [5]. Either scaling is properly described by the ultrasoft gluons of pNRQCD, since they are defined as the ones having all four-momenta much smaller than the soft scale $\sim m\alpha_s$ (UV cutoff), which is satisfied in both cases. However, if one insisted on assigning to the ultrasoft gluons a momentum scaling $m(\lambda^2,\lambda^2,\lambda^2)$ and not smaller (i.e., one is introducing an IR cutoff for them), then the situation $m\alpha_s^4 \sim M(1-z)$ would require the introduction of new (ultra)soft-collinear modes scaling like $m(\lambda^4,\lambda^2,\lambda^3)$ with an UV cutoff $\sim m\lambda^2$ for the $+$ and $\perp$ components. Whether it is convenient or not to make such a splitting is a matter of debate [5,8].

The case $m\alpha_s \sim M(1-z)$ has not been discussed. For the color octet contributions, it requires a calculation in NRQCD, since if one attempts to do it from Fig. 1 one immediately realizes that the four-momentum of the ultrasoft gluon is $\sim m\alpha_s$, a region where pNRQCD is not applicable. Hence at the NRQCD+SCET$_{\rm I}$ level (Sec. II A) one should calculate a set of diagrams involving a collinear and a soft gluon. The leading order contribution comes from the S-wave current only and we have seen it vanish.

We have refrained from putting forward a Lagrangian for the SCET which also holds for heavy quarkonium systems because several issues, like the remarks made above, should be better understood. Clearly, as we have shown in this paper, one cannot simply take over the SCET for heavy-light systems and apply it to heavy quarkonium (for instance, one misses logs which depend on the binding effects). Our analysis also indicates that it may be convenient to rephrase SCET in terms of cutoffs rather than in terms of scaling properties of the various modes as has been done so far. Then, one

would have to account properly for both the suitable cutoffs of pNRQCD and those of SCET.

V. CONCLUSIONS

Apart from making a few remarks, which we hope will be useful for an eventual construction of a SCET Lagrangian adapted to heavy quarkonium systems, we have calculated the *S*- and *P*-wave octet shape functions in the weak coupling regime. We have also discussed their scale dependence. The addition of these contributions to the ones obtained in [11] makes the agreement with data for the end-point photon spectrum of inclusive $\Upsilon(1S)$ decays almost perfect. As a by-product the NRQCD matrix elements $\langle\Upsilon(1S)|O_8(^1S_0)|\Upsilon(1S)\rangle$ and $\langle\Upsilon(1S)|O_8(^3P_J)|\Upsilon(1S)\rangle$ have also been calculated, in the weak coupling regime (see the Appendix) and their scale dependence discussed.

ACKNOWLEDGMENTS

We have benefited from informative discussions on SCET with C. Bauer, T. Becher, M. Beneke, S. Fleming, T. Mehen, M. Neubert, and I. Stewart. J.S. acknowledges the Benasque Center of Physics program ''Pushing the Limits of QCD,'' and P. Bedaque for the opportunity to participate in the ''Effective Summer in Berkeley,'' where some of these discussions took place. Thanks are also given to D. Besson for providing the data of Ref. [12] and to Ll. Garrido for his help in handling it. Finally, we thank A. Penin, and especially A. Pineda, for useful discussions on the Appendix. We acknowledge financial support from a CICYT-INFN collaboration contract, the MCyT and Feder (Spain) grant FPA2001-3598, the CIRIT (Catalonia) grant 2001SGR-00065, and the network EURIDICE (EU) HPRN-CT2002-00311. X.G.T. acknowledges financial support from the Departament d'Universitats, Recerca i Societat de la Informació of the Generalitat de Catalunya.

APPENDIX: CALCULATION OF $\Upsilon(1S)$ NRQCD COLOR OCTET MATRIX ELEMENTS

The calculation in Sec. II C can be easily taken over to provide a calculation of $\langle\Upsilon(1S)|O_8(^1S_0)|\Upsilon(1S)\rangle$ and $\langle\Upsilon(1S)|O_8(^3P_J)|\Upsilon(1S)\rangle$, assuming that $m\alpha_s^2 \gg \Lambda_{\rm QCD}$ is a reasonable approximation for this system. Indeed, we only have to drop the delta function (which requires a further integration over k_+) and arrange for the suitable factors in Eqs. (13) and (14). We obtain

$$\langle\Upsilon(1S)|O_8(^1S_0)|\Upsilon(1S)\rangle = -2T_F^2(N_c^2-1)\int_0^\infty dk_+ S_S(k_+),$$

$$\langle\Upsilon(1S)|O_8(^3P_J)|\Upsilon(1S)\rangle = -\frac{4(2J+1)T_F^2(N_c^2-1)}{3} \times \int_0^\infty dk_+ S_{P1}(k_+), \qquad \text{(A1)}$$

where we have used

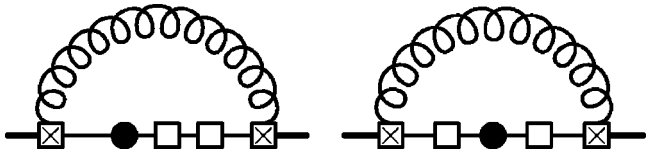

FIG. 5. Diagrams which require a $\mathcal{P}_1(^3S_1)$ operator for renormalization. The solid circle stands for either the $O_8(^1S_0)$ or $O_8(^3P_J)$ operator, the crossed box for either the chromomagnetic (✤) or chromoelectric (❶) interaction in Fig. 1, the empty box for the octet Coulomb potential, and the thin solid lines for free $Q\bar{Q}$ propagators.

$$\int_0^\infty dk_+ S_{P2}(k_+) = \frac{2}{3}\int_0^\infty dk_+ S_{P1}(k_+). \qquad \text{(A2)}$$

The expressions above contain UV divergences which may be regulated in the same way as in Sec. II C, namely, by calculating the ultrasoft loop in D dimensions. These divergences can be traced back to the diagrams in Fig. 5 and Fig. 6. Indeed, if we expand I_S and I_P for large z', we obtain

$$I_S \sim m\sqrt{\frac{\gamma}{\pi}}\frac{\alpha_s N_c}{2}\left\{\frac{1}{z'}+\frac{1}{z'^2}(-1+2\lambda\ln 2) + \frac{1}{z'^3}\left(1-2\lambda+\frac{\lambda^2\pi^2}{6}\right)+\frac{1}{z'^4}\left(-1+\lambda(2\ln 2+1) + \lambda^2(-4\ln 2)+\frac{3}{2}\zeta(3)\lambda^3\right)+\mathcal{O}\left(\frac{1}{z'^5}\right)\right\}, \qquad \text{(A3)}$$

$$I_P \sim \sqrt{\frac{\gamma^3}{\pi}}\frac{8}{3}(2-\lambda)\left\{\frac{1}{2z'}+\left[-\frac{3}{4}+\lambda\left(-\frac{1}{4}+\ln 2\right)\right]\frac{1}{z'^2} + \left(1-\lambda+\frac{1}{12}(-6+\pi^2)\lambda^2\right)\frac{1}{z'^3} + \frac{1}{4}\{-5+\lambda+\lambda^2(2-8\ln 2)+8\lambda\ln 2 + \lambda^3[-4\ln 2+3\zeta(3)]\}\frac{1}{z'^4}+\mathcal{O}\left(\frac{1}{z'^5}\right)\right\}. \qquad \text{(A4)}$$

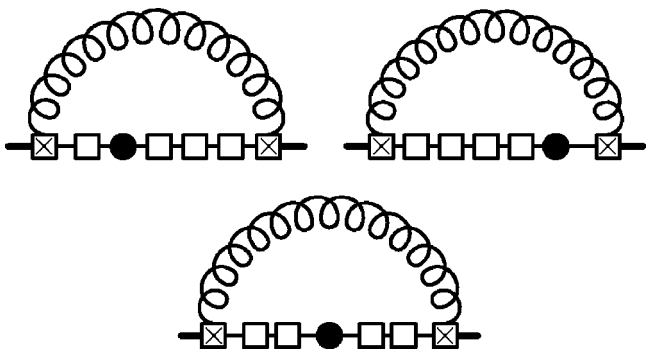

FIG. 6. Diagrams which require a $O_1(^3S_1)$ operator for renormalization. Symbols are as in Fig. 5.

It is easy to see that only powers of $1/z'$ up to order 4 may give rise to divergences. Moreover, each power of $1/z'$ corresponds to one Coulomb exchange. Taking into account the result of the integral

$$\int_0^\infty dk_+ \int_0^\infty dx (2k_+ x)^{-\varepsilon} \frac{1}{z'^\alpha} = 2^{1-2\varepsilon} \left(\frac{\gamma^2}{m}\right)^{2-2\varepsilon} \frac{\Gamma^2(1-\varepsilon)}{\Gamma(\alpha/2)} \Gamma\left(\frac{\alpha}{2}+2\varepsilon-2\right), \quad \text{(A5)}$$

we see that only the $1/z'^2$ and $1/z'^4$ terms produce divergences. The former correspond to diagrams in Fig. 5 and the latter to Fig. 6, which can be renormalized by the operators $\mathcal{P}_1(^3S_1)$ and $O_1(^3S_1)$, respectively. It is again important to notice that these divergences are a combined effect of the ultrasoft loop and quantum mechanics perturbation theory (*potential* loops [33]), and hence it may not be clear at first sight if they must be understood as ultrasoft (producing $\log \mu_u$ in the notation of Refs. [28,29]) or potential (producing $\log \mu_p$ in the notation of Refs. [28,29]). In any case, the logarithms they produce depend on the regularization and renormalization scheme used for both ultrasoft and potential loops. Notice that the scheme we use in this work is not the standard one in pNRQCD [17,28,34]. In the standard scheme the ultrasoft divergences (anomalous dimensions) are identified by dimensionally regulating both ultrasoft and potential loops and subsequently taking $D \to 4$ in the ultrasoft loop divergences only. If we did this in the present calculation we would obtain no ultrasoft divergence. Hence, in the standard scheme there would be contributions to the potential anomalous dimensions only. The singular pieces in our scheme are displayed below:

$$\begin{aligned}
&\langle \Upsilon(1S)|O_8(^1S_0)|\Upsilon(1S)\rangle|_{\varepsilon\to 0} \\
&\simeq -\frac{1}{\varepsilon}\left(\frac{2\gamma^2}{\mu m}\right)^{-2\varepsilon} \frac{1}{24} C_F^2 N_c \alpha_s(\mu_u) [C_f \alpha_s(\mu_s)]^4 \frac{\gamma^3}{\pi^2} \\
&\quad \times \left(2 + \lambda[-7 - 4\log 2] \right. \\
&\quad + \lambda^2 \left[4 + 8\log 2 + 4\log^2 2 + \frac{\pi^2}{3} \right] \\
&\quad \left. + \lambda^3 \left[-4\log^2 2 - \frac{\pi^2}{3} - \frac{3}{2}\zeta(3) \right] \right), \\
&\langle \Upsilon(1S)|O_8(^3P_J)|\Upsilon(1S)\rangle|_{\varepsilon\to 0} \\
&\simeq -(2J+1)\frac{1}{\varepsilon}\left(\frac{2\gamma^2}{\mu m}\right)^{-2\varepsilon} \frac{4}{27} C_f \alpha_s(\mu_u) \\
&\quad \times [C_f \alpha_s(\mu_s)]^2 \frac{\gamma^5}{\pi^2} (2-\lambda) \left(-4 + + \lambda \left[\frac{47}{12} + 5\log 2 \right] \right. \\
&\quad + \lambda^2 \left[\frac{5}{6} - \frac{2\pi^2}{9} - \frac{8}{3}\log 2 - \frac{8}{3}\log^2 2 \right] \\
&\quad \left. + \lambda^3 \left[-\frac{7}{12} + \frac{\pi^2}{9} - \frac{5}{3}\log 2 + \frac{4}{3}\log^2 2 + \frac{3}{4}\zeta(3) \right] \right).
\end{aligned} \quad \text{(A6)}$$

[1] M.J. Dugan and B. Grinstein, Phys. Lett. B **255**, 583 (1991).
[2] C.W. Bauer, S. Fleming, and M.E. Luke, Phys. Rev. D **63**, 014006 (2001).
[3] C.W. Bauer, S. Fleming, D. Pirjol, and I.W. Stewart, Phys. Rev. D **63**, 114020 (2001); C.W. Bauer and I.W. Stewart, Phys. Lett. B **516**, 134 (2001); C.W. Bauer, D. Pirjol, and I.W. Stewart, Phys. Rev. D **65**, 054022 (2002); **66**, 054005 (2002); **68**, 034021 (2003); D. Pirjol and I.W. Stewart, *ibid.* **67**, 094005 (2003).
[4] M. Beneke, A.P. Chapovsky, M. Diehl, and T. Feldmann, Nucl. Phys. **B643**, 431 (2002); M. Beneke and T. Feldmann, Phys. Lett. B **553**, 267 (2003).
[5] R.J. Hill and M. Neubert, Nucl. Phys. **B657**, 229 (2003); T. Becher, R.J. Hill, and M. Neubert, hep-ph/0308122; T. Becher, R.J. Hill, B.O. Lange, and M. Neubert, Phys. Rev. D **69**, 034013 (2004).
[6] M. Beneke, http://wwwteor.mi.infn.it/~brambill/school.html; M. Neubert, *ibid.*
[7] C.W. Bauer, S. Fleming, D. Pirjol, I.Z. Rothstein, and I.W. Stewart, Phys. Rev. D **66**, 014017 (2002).
[8] M. Beneke and T. Feldmann, hep-ph/0311335; B.O. Lange and M. Neubert, hep-ph/0311345; C.W. Bauer, M.P. Dorsten, and M.P. Salem, hep-ph/0312302; J. Chay and C. Kim, hep-ph/0401089.
[9] C.W. Bauer, C.W. Chiang, S. Fleming, A.K. Leibovich, and I. Low, Phys. Rev. D **64**, 114014 (2001).
[10] S. Fleming and A.K. Leibovich, Phys. Rev. Lett. **90**, 032001 (2003).
[11] S. Fleming and A.K. Leibovich, Phys. Rev. D **67**, 074035 (2003).
[12] CLEO Collaboration, B. Nemati *et al.*, Phys. Rev. D **55**, 5273 (1997).
[13] S.J. Brodsky, D.G. Coyne, T.A. DeGrand, and R.R. Horgan, Phys. Lett. **73B**, 203 (1978); D.M. Photiadis, *ibid.* **164B**, 160 (1985); S. Wolf, Phys. Rev. D **63**, 074020 (2001).
[14] A.L. Kagan and M. Neubert, Eur. Phys. J. C **7**, 5 (1999); F. De Fazio and M. Neubert, J. High Energy Phys. **06**, 017 (1999).
[15] S. Titard and F.J. Yndurain, Phys. Rev. D **49**, 6007 (1994); **51**, 6348 (1995); Phys. Lett. B **351**, 541 (1995); A. Pineda and F.J. Yndurain, Phys. Rev. D **58**, 094022 (1998); **61**, 077505 (2000); A. Pineda, J. High Energy Phys. **06**, 022 (2001).
[16] N. Brambilla, Y. Sumino, and A. Vairo, Phys. Lett. B **513**, 381 (2001); Phys. Rev. D **65**, 034001 (2002); S. Recksiegel and Y. Sumino, *ibid.* **67**, 014004 (2003).
[17] B.A. Kniehl, A.A. Penin, V.A. Smirnov, and M. Steinhauser, Nucl. Phys. **B635**, 357 (2002); A.A. Penin and M. Steinhauser, Phys. Lett. B **538**, 335 (2002).

[18] B.A. Kniehl, A.A. Penin, A. Pineda, V.A. Smirnov, and M. Steinhauser, hep-ph/0312086.
[19] B.A. Kniehl, A.A. Penin, M. Steinhauser, and V.A. Smirnov, Phys. Rev. Lett. **90**, 212001 (2003).
[20] G.T. Bodwin, E. Braaten, and G.P. Lepage, Phys. Rev. D **51**, 1125 (1995); **55**, 5853(E) (1997).
[21] A. Pineda and J. Soto, Nucl. Phys. B (Proc. Suppl.) **64**, 428 (1998); N. Brambilla, A. Pineda, J. Soto, and A. Vairo, Nucl. Phys. **B566**, 275 (2000).
[22] I.Z. Rothstein and M.B. Wise, Phys. Lett. B **402**, 346 (1997).
[23] F. Maltoni and A. Petrelli, Phys. Rev. D **59**, 074006 (1999).
[24] M. Kramer, Phys. Rev. D **60**, 111503 (1999).
[25] N. Brambilla, D. Eiras, A. Pineda, J. Soto, and A. Vairo, Phys. Rev. D **67**, 034018 (2003).
[26] M. Beneke, G.A. Schuler, and S. Wolf, Phys. Rev. D **62**, 034004 (2000).
[27] M.E. Luke, A.V. Manohar, and I.Z. Rothstein, Phys. Rev. D **61**, 074025 (2000).
[28] A. Pineda, Phys. Rev. D **65**, 074007 (2002); Phys. Rev. A **66**, 062108 (2002).
[29] A. Pineda, Phys. Rev. D **66**, 054022 (2002).
[30] F. Hautmann, Nucl. Phys. **B604**, 391 (2001).
[31] A.V. Manohar, J. Soto, and I.W. Stewart, Phys. Lett. B **486**, 400 (2000).
[32] J.H. Field, Phys. Rev. D **66**, 013013 (2002).
[33] M. Beneke and V.A. Smirnov, Nucl. Phys. **B522**, 321 (1998).
[34] A. Pineda and J. Soto, Phys. Lett. B **420**, 391 (1998); Phys. Rev. D **59**, 016005 (1999).